Three-dimensional plasmoid-mediated reconnection and the effect of toroidal guide field in simulations of coaxial helicity injection

Cite as: Phys. Plasmas **26**, 092502 (2019); https://doi.org/10.1063/1.5098482
Submitted: 02 April 2019 . Accepted: 10 August 2019 . Published Online: 03 September 2019

F. Ebrahimi

Physics of Plasmas ARTICLE scitation.org/journal/php

Three-dimensional plasmoid-mediated reconnection and the effect of toroidal guide field in simulations of coaxial helicity injection

Cite as: Phys. Plasmas **26**, 092502 (2019); doi: 10.1063/1.5098482
Submitted: 2 April 2019 · Accepted: 10 August 2019 ·
Published Online: 3 September 2019

F. Ebrahimi

AFFILIATIONS

Princeton Plasma Physics Laboratory, and the Department of Astrophysical Sciences, Princeton University, Princeton, New Jersey 08544, USA

Note: This paper is part of the Special Collection: Advances in Magnetic Reconnection Research in Space and Laboratory Plasmas. Part IV.

ABSTRACT

Physics of three-dimensional plasmoid-mediated magnetic reconnection during transient Coaxial Helicity Injection (CHI) plasma start-up is investigated using nonlinear MHD simulations in a spherical tokamak. We numerically examine (i) the role of three-dimensional magnetic fluctuations arising from current-sheet instabilities on the formation of plasmoid-mediated closed flux surfaces, and (ii) the effect of toroidal guide field on the MHD stability during transient CHI. We find that even in the presence of nonaxisymmetric edge magnetic fluctuations, current-carrying axisymmetric ($n = 0$) plasmoids are rapidly formed while twisted open field lines are being injected and are merged to form a large current-carrying magnetic bubble for plasma startup in a tokamak. It is also found that the 3-D physics response is drastically different for simulations at a higher toroidal field, and complete stabilization of nonaxisymmetric fluctuations was achieved at a higher toroidal flux.

I. INTRODUCTION

The observed twistedness of magnetic field lines in nature is usually expressed as a global quantity, magnetic helicity.[1–3] In magnetically dominated plasmas, such as the solar corona region, magnetic helicity can be injected through twisting field lines via shear motion of their foot points.[4,5] The injected magnetic fields can, however, be annihilated through the process of magnetic reconnection, i.e., the rearrangement of magnetic field topology of plasmas. The twisting of the field lines during helicity injection can bring the oppositely directed field lines together to form current sheets and cause magnetic reconnection. In laboratory confined plasmas, magnetic helicity can also be injected through driving current along open field lines, to form current-carrying bubbles, so-called reconnecting plasmoids.[6] In particular, various magnetic helicity techniques are generally utilized for current-drive in toroidal magnetic fusion configurations. Similarly, the injection of twisted magnetic field lines for current drive in toroidal configurations is usually accompanied by magnetic reconnection. For an optimal current drive during helicity injection, understanding the process of magnetic reconnection is therefore critical.

Conventional current-drive techniques in magnetically confined tokamaks are inductive, i.e., they rely on the current ramp-up in the primary coil or a central solenoid to produce an electric field. These techniques cannot be steady-state. For feasible fusion reactors, noninductive current-drive techniques, such as various innovative helicity injection techniques and subsequent RF- or neutral-beam injection, are essential for steady-state operation. Elimination of the large central solenoid component required for inductive techniques is also desirable in advanced tokamaks, in particular, for compact reactor designs based on the spherical tokamak. In spherical tokamaks, due to the limited space for a central solenoid, full noninductive current drive is one of the primary objectives to make this configuration reactor relevant. In this paper, we present three-dimensional MHD simulation results for a particular type of helicity-injection technique, the so-called transient coaxial helicity injection (CHI). The key role of plasmoid-mediated magnetic reconnection will be demonstrated during helicity injection for noninductive plasma startup current formation in a spherical tokamak.

Helicity injection as a form of noninductive current-drive technique has been utilized in various fusion configurations, including tokamaks, spherical tokamaks, reversed-field pinches, and spheromaks.[7–12] Magnetic helicity through "the linkage of magnetic fluxes" could steadily be injected into the plasma to form and sustain a configuration against the resistive decay. Among various forms of helicity injection techniques, CHI, a form of electrostatic helicity injection, has been successfully used to form spheromaks[13] and spherical

tokamaks.[14] In these configurations during driven CHI, nonaxisymmetric instabilities have the role of transporting current from the edge to the core via a dynamo relaxation process. However, in another form of CHI, the so-called "transient" CHI, the primary goal is to form a startup current in the absence of any nonaxisymmetric magnetic fluctuations, i.e., without any types of current-driven instabilities. Transient CHI, developed on the HIT-II experiment,[15] has been the leading candidate for solenoid-free plasma start-up in the National Spherical Torus Experiment (NSTX) and NSTX-U. In NSTX, transient CHI has generated over 200 kA of toroidal current on closed flux surfaces without the use of the conventional central solenoid.[16,17] Further transient CHI experiments have recently been conducted in the Q-shu University Experiment with Steady State Spherical Tokamak (QUEST) device[18] and are expected to begin for full noninductive current drive on the Unified Reduced Non-Inductive Assessment (URANIA) device (formerly PEGASUS) at the University of Wisconsin.

In transient CHI, magnetic reconnection plays a pivotal role for successful plasma current startup.[6,19–21] Transient CHI starts with an initial poloidal flux, the injector flux (Ψ_{inj}), which is produced by the lower poloidal coils (called injector and flux-shaping coils). In the presence of a toroidal field, a constant voltage (V_{inj}) is then applied to the lower divertor plates to drive current along the open field lines (Fig. 1). Helicity is injected through the linkage of resulting toroidal flux with the poloidal injector flux, with the rate of helicity injection being twice the product of injector flux and voltage. Plasma and open field lines expand into the vessel when the Lorentz force $J_{pol} \times B_{tor}$ exceeds the field line tension of the injector flux. For optimal plasma start-up, the injected poloidal flux has to form closed flux surfaces via magnetic reconnection, i.e., the injected open field lines ought to reconnect in the injection region, where the footprint of initial open field connects the two lower plates in the device. The newly formed closed field lines give rise to toroidal plasma current in the closed flux region. It is therefore important to understand the fundamental reconnection mechanism that leads to the generation of closed flux surfaces during transient CHI. It should be noted that the process of magnetic reconnection during magnetic helicity injection here is similar to the reconnection process in some natural plasmas. Here, the helicity is injected through driving current along open field lines, while in natural plasmas, such as on the surface of the sun, magnetic helicity could be injected through twisting field lines via shear motion of their foot points.

The process of magnetic reconnection during CHI in NSTX/NSTX-U has been extensively studied using axisymmetric global resistive MHD simulations in toroidal geometry. As shown in Fig. 2, it has been demonstrated that reconnection is induced through two mechanisms when (1) the oppositely directed field lines in the injector region are forced to reconnect after the injector current is rapidly reduced to zero and a stable Sweet-Parker (S-P) current sheet forms—"forced reconnection" [Fig. 2(a)[19,20]] (2) at high Lundquist number, the elongated current sheet becomes MHD unstable due to the plasmoid instability[6,22–26]—"spontaneous reconnection" [Fig. 2(b)]. The latter is a rare classical example of 2-D plasmoid formation in a large-scale fusion plasma, which was demonstrated through nonlinear global resistive MHD simulations using the NIMROD code.[6] The transition to plasmoid instability was shown to occur when the local Lundquist number $S = LV_A/\eta$ (V_A is the Alfvén velocity based on the poloidal reconnecting magnetic field, L is the current sheet length, and η is the magnetic diffusivity) exceeded 3000 (above a critical current sheet aspect ratio of ~70). Note that by including the toroidal guide field in the Lundquist number, the transition could be at a much higher global

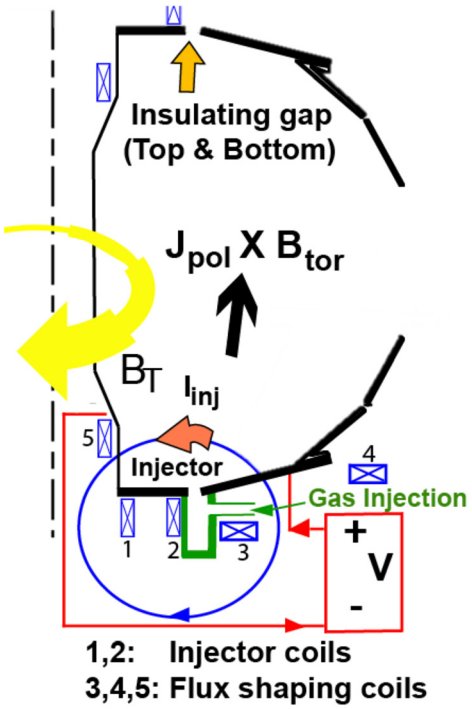

FIG. 1. Magnetic helicity injection in the laboratory. Provided injected poloidal flux (blue circle) generated by poloidal-field coils located in the lower divertor region under the device [primary injector coil (PF1CL) and the flux shaping coils (PF2L and PF1AL)], current is applied along open field lines in the presence of a large toroidal guide field (B_T). The injected toroidal flux from poloidal current along the field lines is linked with the injected poloidal flux.

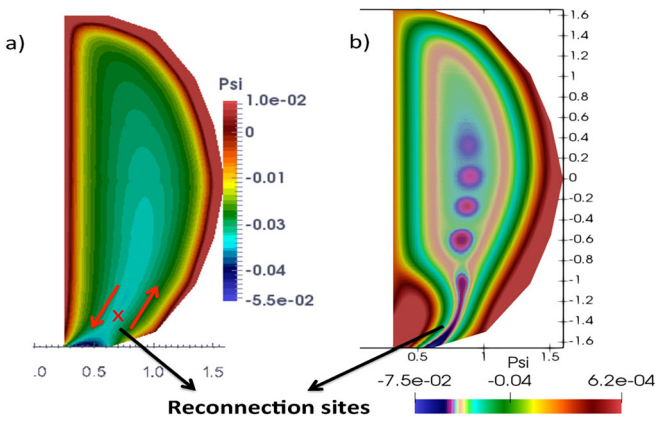

FIG. 2. Poloidal flux (Wb) during (a) decay phase of simulations with wide footprint in NSTX configuration when the injector voltage is turned off to induce a forced reconnection around the injection region, (b) driven (injection) phase of simulations with narrow footprint in NSTX-U configuration while the injector voltage (V_{inj}) is still applied—reconnection occurs due to a spontaneous plasmoid instability. The arrows and cross show the oppositely directed field lines and x point, respectively.

S. In a global geometry, for the first time, these simulations showed that reconnection rate could increase during plasmoid-mediated reconnection "in the presence of toroidal guide field."[6] These simulations in realistic experimental geometry motivated a search for the experimental evidence of plasmoids in the NSTX transient CHI plasmas, and detailed experimental analysis indeed found evidence of the predicted plasmoid formation in NSTX camera images. This observation is the first qualitative experimental evidence of plasmoid formation in a laboratory fusion device.[6]

The physics of 3-D reconnection during helicity injection was also examined, and it was found that in multi-current-sheet configurations, self-consistent 3-D magnetic fluctuations arising from neighboring outer current sheets can trigger plasmoid instability in the primary inner current sheet.[27] This effect, which is absent in 2-D, was explained in terms of local dynamo flux amplification in 3-D turbulent plasma. It was shown that field amplification from 3-D effects enhances the local Lundquist number to trigger plasmoid instability and therefore is an important factor in the onset of reconnection, the so-called trigger problem. In 3-D, time-evolving edge current sheets, which were identified during nonlinear three-dimensional MHD simulations,[27] were also shown to cause reconnecting edge localized peeling-type instabilities[28] and be important in transient Vertical Displacement Events (VDEs). Edge 3-D current-sheet instabilities for the first time were shown (i) to grow on the poloidal Alfvénic time scales and break the axisymmetric current,[27] and (ii) to cause the formation of edge current-driven peeling filaments, which do relax due to fluctuation-induced dynamo term.[28]

In this paper, we numerically examine the 3-D MHD stability and current formation for an optimal plasma startup and achieve a large-volume closed flux surfaces during CHI. Our previous axisymmetric resistive MHD simulations have been able to show large-fraction conversion of injected open flux to closed flux in the NSTX-U geometry.[21] Here, three-dimensional MHD NIMROD simulations have been carried out to further investigate two major effects: (1) the role of 3-D magnetic fluctuations arising from $n \neq 0$ current-sheet instabilities on the formation of plasmoid-mediated closed flux surfaces, and (2) the effect of toroidal field on the 3-D stability during transient CHI. Closed flux current of about 220 kA and large-volume closed flux surfaces are obtained even in the presence of nonaxisymmetric edge magnetic fluctuations. Although the current-driven single mode n = 1 activity has been shown to trigger during strongly driven helicity injection,[29,30] here, we find that the 3-D physics response is drastically different for simulations at a higher toroidal field, and complete stabilization of $n \neq 0$ nonaxisymmetric fluctuations is achieved at a higher toroidal flux. In Sec. II, we present the details of the model we used in the simulations. In Sec. III, the results from 3-D simulations for both examining the effect of nonaxisymmetric perturbations and toroidal magnetic field will be presented. We summarize in Sec. IV.

II. THE MODEL

To study the very dynamical process of helicity injection and the formation of closed flux surfaces during CHI, we perform three-dimensional time-dependent resistive MHD simulations using the NIMROD code.[31] Our simulations are performed for a zero-pressure model (pressure is not evolved in time) with constant in time poloidal-field coil currents to generate the injector and shaping fluxes (fixed boundary-flux simulations). Similar to our earlier axisymmetric simulations, and similar to the experiment, the simulations start with an initial poloidal field generated by poloidal-coil currents in the primary injector coil (PF1CL, coil number 2 in Fig. 1 is energized here) and the flux-shaping coils (PF2L and PF1AL, coil numbers 3 and 5 in Fig. 1 are energized here). In the presence of a toroidal field, a constant electric field is applied across the narrow injector gap (at Z = −1.65 m). Perfectly conducting boundary conditions with no-slip are used, except at the injector gap, which has a normal $E \times B$ flow where a constant-in-time electric field is applied.[19,32] We use a poloidal grid with 45×90 fifth-order finite elements in a global (R,Z) geometry and toroidal mode numbers up to 43 modes. A uniform number density of 4×10^{18} m^{-3} for a deuterium plasma is used.

Plasmoid-mediated magnetic reconnection process is studied during two phases of driven (injection) and decay of transient CHI. Our simulations are performed during both phases, starting with injection phase when the injector voltage is applied, and in the decay phase, when the applied voltage at the gap is turned off after the injected flux has fully expanded into the volume. As has been demonstrated by our earlier simulations in the NSTX and NSTX-U configurations, magnetic reconnection can occur in both phases. By optimizing the locations of injector flux and flux shaping coils, a better shaping of the initial flux and narrower injector-flux footprints were obtained in the NSTX-U simulations.[21] As a result, with narrow flux footprint, the local Lundquist number can be higher (due to the higher accumulation of reconnecting B_z field in the injection region and the formation of a longer current sheet), to facilitate a transition to plasmoid instability and reconnection in the injection region.[6,21] The oppositely directed field lines in the injector region could also be forced to reconnect through a local Sweet-Parker type reconnection during the decay phase. As the injector voltage is turned off, magnetic field compression exerts a radial $\mathbf{J} \times \mathbf{B}$ that causes reconnection.[19,20] Our simulations here are in the configuration with narrow injector-flux footprints [Fig. 2(b)], and plasmoid-mediated reconnection occurs during both injection phase (when the injector voltage is applied) and the decay phase (when the injector voltage is turned off). Below, we present the results of 3-D simulations to examine the effect of both nonaxisymmetric fluctuations, as well as the effect of toroidal magnetic field.

III. THREE-DIMENSIONAL RESULTS

A. The onset of 3-D current-sheet instabilities and the effect of nonaxisymmetric perturbations

Earlier nonlinear resistive MHD simulations in the absence of three-dimensional fluctuations have demonstrated a large volume of closed flux surfaces with narrow injector-flux footprint during transient CHI in NSTX-U configuration.[21] Here, we examine whether the formation of maximum volume closed flux surfaces during transient CHI is feasible in the presence of nonaxisymmetric 3-D magnetic fluctuations. We perform full 3-D simulations in NSTX-U geometry with a toroidal field of $B_\phi = 1.23$ T. The poloidal-coil current is adjusted to produce an initial injector flux with narrow footprint. Strong flux-shaping coils with currents PF1AL = −180 kA turns and PF2L = −5 kA turns are used, and the current in the primary injector coil (PF1CL) is 140 kA turns. As shown in Fig. 2(b), the narrow-footprint injector flux is expanded to fill up the volume during helicity injection, while a constant injector voltage is applied. The local Lundquist number is high enough to allow reconnection through plasmoid instability. We investigate the effect of 3-D nonaxisymmetric perturbations during both injection and decay phases.

Helicity injection in the simulations starts by applying a constant voltage.

Figure 3 shows the total energy vs time during the full nonlinear 3-D simulation. During helicity injection, the injected poloidal flux fills up the vessel to give a total current of 320 kA, as shown in Fig. 3(b). Axisymmetric edge toroidal current layers (with a peak current density of $J_\phi = 420\ \mathrm{kA/m^2}$) are formed poloidally (on both low-field and high-field sides). Total plasma current is not affected by the presence of nonaxisymmetric fluctuations in 3-D, and similar currents are obtained in 3-D and 2-D simulations [Fig. 3(b)]. As seen from the magnetic energy in Fig. 3(a), low-n nonaxisymmetric modes are triggered. These instabilities grow as the flux expands into the device and the plasma current evolves. The nature of these current-driven instabilities can be examined through the evolution of the current density profiles. The poloidal R-Z cross section of toroidal current densities is shown in Fig. 4 during the growth phase of these instabilities, at t = 6.6 ms, and later in time at t = 8.7 ms. It is shown that two types of current sheets are formed during helicity injection.[27] A primary inner current sheet in the injection region, which is responsible for global 2-D plasmoid reconnection and the formation of the closed flux region. As the poloidal field vanishes in the injection region (reconnection site), this primary inner current sheet can become unstable to 2-D n = 0 plasmoid instability and breaks into magnetic islands (plasmoids), as shown in Fig. 4(b). A secondary outer current sheet due to the accumulation of flux in the edge region can also form as the flux expands. This outer current sheet, however, can be unstable to 3-D current-sheet instabilities, i.e., the nonaxisymmetric ($n \neq 0$) reconnecting current-driven instability.

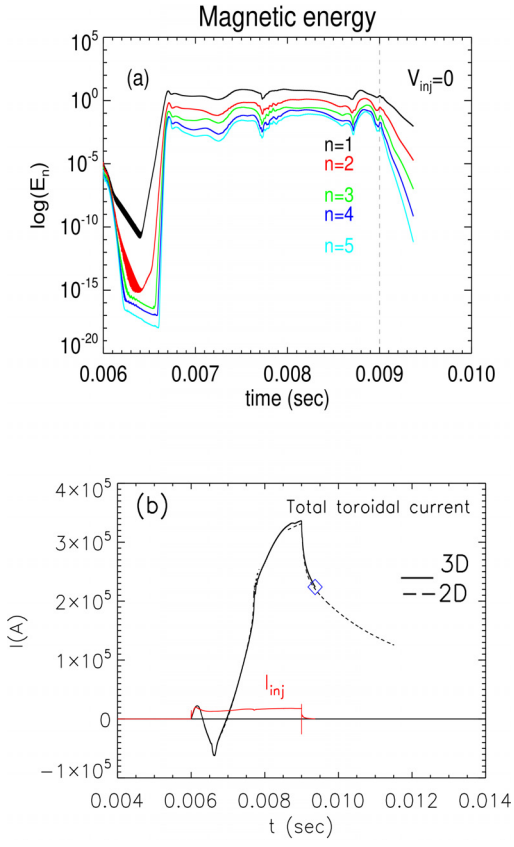

FIG. 3. 3-D nonlinear simulations in a toroidal spherical tokamak geometry with $B_\phi = 1.23$ T. (a) Total magnetic energies of different toroidal mode numbers vs time (in seconds). (b) Toroidal plasma current and injector current (in red) vs time. The closed flux current is about $I_p \sim 220$ kA.

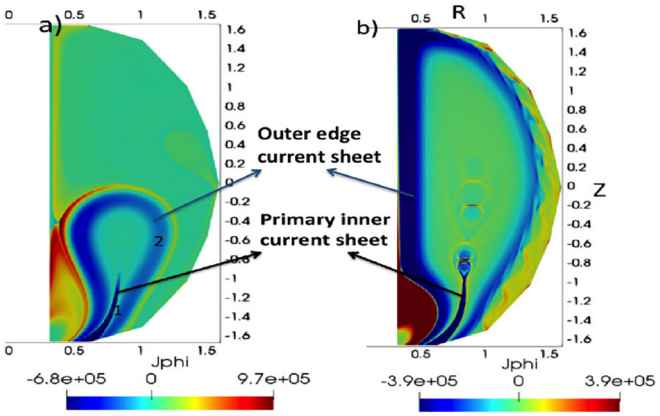

FIG. 4. Time-evolving current sheets during flux expansion: (1) primary inner current sheet, where reconnecting n = 0 plasmoids form; and (2) outer edge current sheet, where nonaxisymmetric edge magnetic fluctuations could excite. Poloidal R-Z cut of the total toroidal current density, J_ϕ (A/m^2), (a) during early expansion at t = 6.6 ms and (b) t = 8.7 ms.

As the length of these time-evolving outer edge current sheets are increased, localized 3-D current-sheet instabilities start to grow. The mode structures reveal further the nature of these current-sheet instabilities. The structures are localized around the current-sheet layers with tearing-like parity, as shown in Fig. 5. The radial magnetic field structure for n = 1 shows, on average, an even parity (in radius) and odd parity for the radial velocity structure. Low-n n = 1–2 are linearly driven as they grow early in time (in the absence of other fluctuations); however, modes with higher n, n = 3, 4 and above grow later in time (when n = 1–2 have already grown to finite amplitudes) with larger growth rates. As the instabilities are localized current-sheet instabilities, we use the relevant poloidal Alfvén time scales and velocities calculated based on the peak reconnecting poloidal field around the edge current layers, $B_z \approx 0.087$ T. The growth rates are $\gamma\tau_{A(n=1)} \sim 0.1$, $\gamma\tau_{A(n=2)} \sim 0.045$, and the local Lundquist number for reconnection is $S = LV_A/\eta \sim 1.2 \times 10^5$. Other low-n modes are driven to grow fast with rates of $\gamma\tau_{A(n=3)} \sim 0.34$, $\gamma\tau_{A(n=4)} \sim 0.45$. These low-n modes saturate at t = 6.7 ms and exhibit relaxation cycles in the nonlinear phase. These modes saturate by modifying and breaking the axisymmetric outer edge current-density layer [see Fig. 4(b)]. Modes with higher n grow to much lower amplitudes (e.g., n = 20 saturates with a magnetic energy of 10^{10}).

After the injected poloidal flux has expanded into the volume in transient CHI, the injector voltage (a contributor to the source term of helicity injection rate $V_{\mathrm{inj}}\Psi_{inj}$) is turned off to force all the remaining injected open field lines to close and form a large-volume closed flux surfaces. As seen in Fig. 3(a), at t = 9 ms during the decay phase ($V_{\mathrm{inj}} = 0$), as the plasma current on the open field lines starts to decay, the amplitudes of nonaxisymmetric modes also start to decay rapidly. We should note that the drop of the total current during the decay

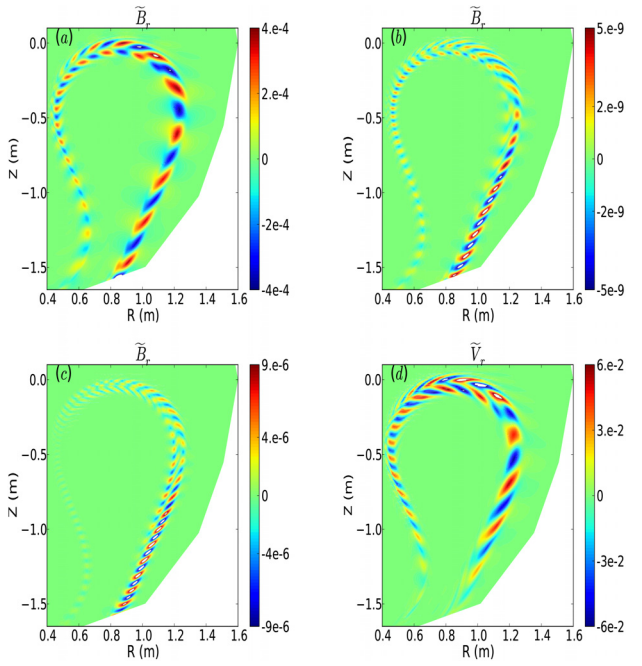

FIG. 5. Radial magnetic field structures: (a) n = 1, (b) n = 2, (c) n = 3, and (d) the radial velocity structure for n = 1 during the growth phase at t = 6.65 ms.

phase largely depends on the plasma temperature, and at higher S with a pressure model, the current decay could be controlled to be smaller.

We next examine the volume of the closed flux surfaces and the enclosed plasma current during the decay phase of transient CHI. Figure 6(a) shows the poloidal closed flux surfaces and the enclosed current density during the decay phase at t = 9.37 ms. As seen, the poloidal flux within the last closed flux surface is 45 mWb and, which is about 65%–70% of the injector flux. It is therefore found that even in the presence of 3-D fluctuations during the injection phase, in transient CHI, a large volume of closed flux surfaces still is feasible as the fluctuations also decay in the decay phase. The poloidal cut of current density showing a closed current supported by an X-point formation remains at an equilibrium state during the decay phase (Fig. 6).

The toroidally averaged poloidal flux closure in three dimensions is not a sufficient indicator to show the absence of stochasticity. Good closed flux surfaces should be confirmed by following the field lines in 3-D. The Poincare plots, the intersections of a field line with a poloidal plane, during 2-D simulations (in the absence of 3-D fluctuations) and at two times during the 3-D simulation are shown in Fig. 7. As seen at t = 9 ms during the injection phase, some open field lines near the injection region have been closed and several islands (five plasmoids in 3-D and four plasmoids in 2-D) have been formed due to plasmoid instability. The number of plasmoids is higher in 3-D case compared to that in the 2-D case. This has also been shown previously[21] that the magnetic fluctuations around the primary inner current sheet could further enhance the reconnection and the formation of plasmoids. The Poincare plots near the edge region, however, show similar intersections for the 2-D and 3-D simulations, as the edge region is mainly dominated by the open field lines during the injection phase in both 3-D and 2-D [Figs. 7(a) and 7(b)]. During the decay phase, the open field lines start to close [Fig. 7(c)], and at t = 9.37 ms, most of the open field lines are closed and a large volume of closed flux surfaces is formed, as seen in the 3-D Poincare plot [Fig. 7(d)]. It is interesting to note that due to MHD dynamical movements, all the axisymmetric small-scale plasmoids formed during the injection phase do merge and form a large-scale current-carrying magnetic bubble (plasmoid). This transition from small-scale plasmoids to large-scale plasmoids in undriven closed plasma (the injector voltage is zero) was also first observed in the axisymmetric simulations.[6] We have calculated the total plasma current in the closed flux region, and a maximum of 228 kA closed flux current is obtained, as shown in Fig. 3(b) (blue diamond). Nearly all of the CHI-generated current is a closed flux current.

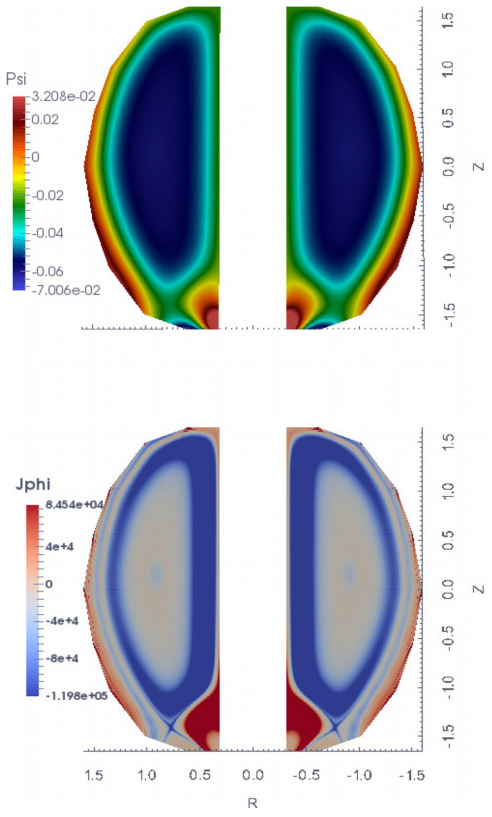

FIG. 6. Formation of large-volume closed flux surfaces during three-dimensional simulations (with time history shown in Fig. 3) of transient CHI at t = 9.37 ms. Poloidal flux (weber) (top) and poloidal R-Z cut of the total toroidal current density, J_ϕ (A/m^2) (bottom).

B. The effect of toroidal guide field in 3-D

In global simulations of plasmoid instability as current sheet became elongated during helicity injection, it was shown that the magnetic reconnection rate becomes nearly independent of Lundquist number and fast reconnection was demonstrated even in the presence of a toroidal guide field ($B_\phi \sim 0.7$ T) in NSTX.[6] Here, we study the effect of the toroidal field on the onset of nonaxisymmetric ($n \neq 0$)

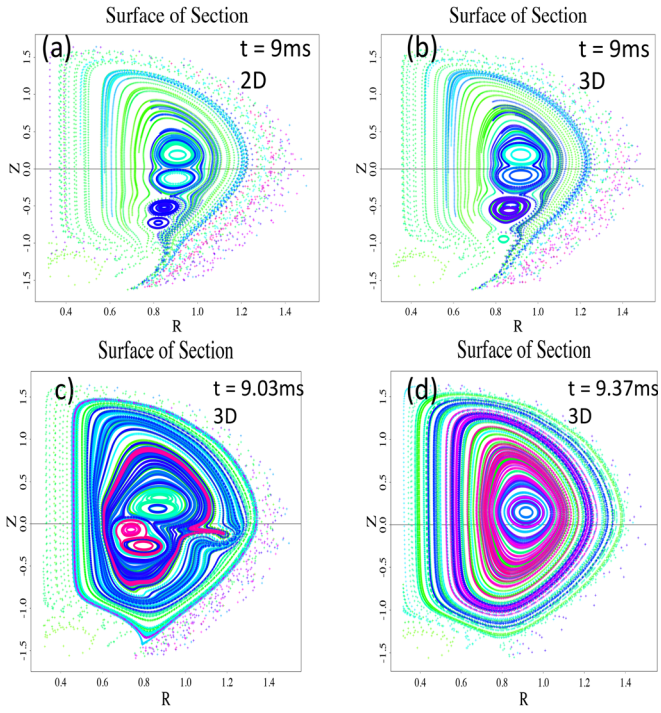

FIG. 7. Poincare plots, the intersections of a field line with a poloidal plane, as the field line is followed around the torus (a) during 2-D simulation (four plasmoids formed) at t = 9 ms during the injection phase, (b)–(d) during 3-D simulation (compare with Fig. 3). (b) At t = 9 ms (five plasmoids formed), (c) at t = 9.03 ms, and (d) at t = 9.37 ms during the decay phase ($V_{inj} = 0$) in 3-D simulations. Small-scale plasmoids merge to form a large-scale plasmoid.

current-sheet instabilities. To examine the effect of toroidal field in the 3-D simulations of transient CHI, we perform two sets of simulations with different toroidal fields. Simulations are performed with the same injector flux used above (Sec. III A), but here, lower injector voltage is used to produce a smaller total current of 220 kA. Also the injector voltage is adjusted to give the same CHI-generated current of 220 kA for both simulations at two toroidal fields ($B_\phi = 1.23$ T and $B_\phi = 2.8$ T, respectively), as shown in Fig. 8(a). Total plasma currents for 2-D (n = 0) simulations and simulations including nonaxisymmetric n = 1, 2 modes remain the same, i.e., the fluctuations do not have a significant effect on the CHI-generated current. The lower panel of Fig. 8 shows the total magnetic energy for two nonaxisymmetric modes vs time. As seen, the nonaxisymmetric n = 1 and n = 2 are stable at a higher toroidal field $B_\phi = 2.8$ T during the full nonlinear simulation. However, at a lower toroidal magnetic field, nonaxisymmetric modes are unstable, and the final growth rate of n = 1 (with $B_\phi = 1.23$ T) is $\gamma\tau_{A(n=1)} \sim 0.06$, which is lower than the linear growth rates for the case in Sec. III, due to lower free energy $J_{||}/B$. The current-driven nonaxisymmetric modes saturate at finite amplitudes, but they do decay during the decay phase [when injection voltage is turned off, as shown in Fig. 8(b)] and would not affect the final closed flux surfaces.

To further investigate the stability of these simulations at two different values of toroidal fields, we examine the nonlinear evolution of the current-density profile. As the injection voltage is adjusted to give the same plasma current for both simulations at two different values

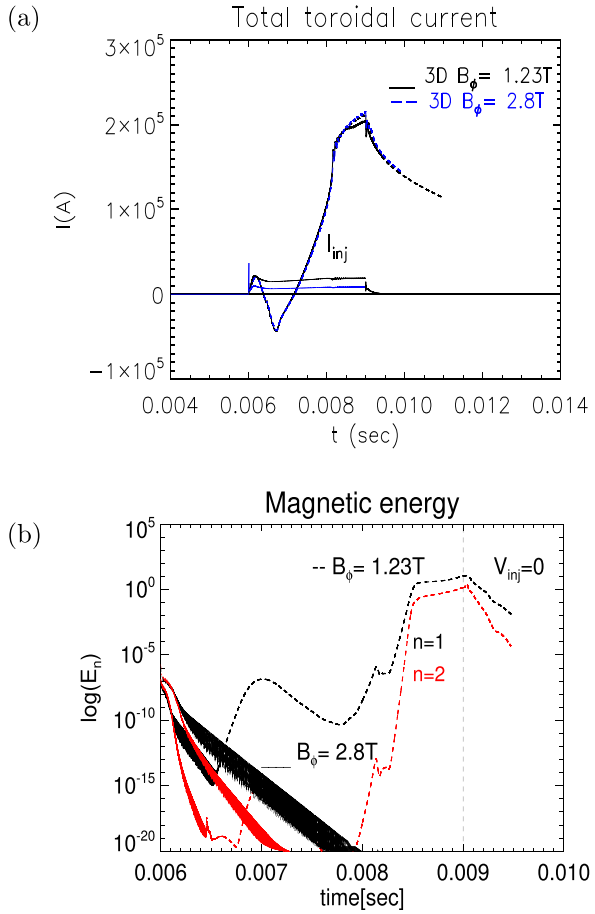

FIG. 8. Simulations with two toroidal magnetic fields, $B_\phi = 1.23$ T, 2.8 T. (a) Toroidal plasma currents and injector currents. Plasma currents overlap for 2-D (n = 0) simulations and simulations including n = 1, 2. The injector voltage is adjusted ($V_{inj} = 1.2$, 2 kV for the two cases of $B_\phi = 1.23$ T, 2.8 T, respectively) to produce the same total plasma current. (b) Total magnetic energies of toroidal mode numbers n = 1, 2 vs time (in seconds) for the two cases of toroidal magnetic fields. The modes are stable for the case with $B_\phi = 2.8$ T.

of toroidal fields, similar current densities are obtained for the two cases, as shown in the top panel of Fig. 9. However, a higher toroidal field case results in lower free energy for current-driven instability in terms of the J_ϕ/B_ϕ profiles (or more generally, parallel current density $\lambda = \mathbf{J}\cdot\mathbf{B}/B^2$). At higher B_ϕ, stability is therefore achieved due to the lower J_ϕ/B_ϕ, as shown in Fig. 9(b).

IV. SUMMARY

In the framework of 3-D global resistive MHD model in toroidal geometry, we have investigated the process of plasmoid-mediated reconnection for plasma startup current formation during transient coaxial helicity injection in a spherical tokamak. Injected open field lines do reconnect while expanding in the volume to produce plasma current. During the magnetic helicity injection process, elongated current sheets can form and could break into magnetic islands (plasmoids) at high Lundquist number. We find that even in the presence

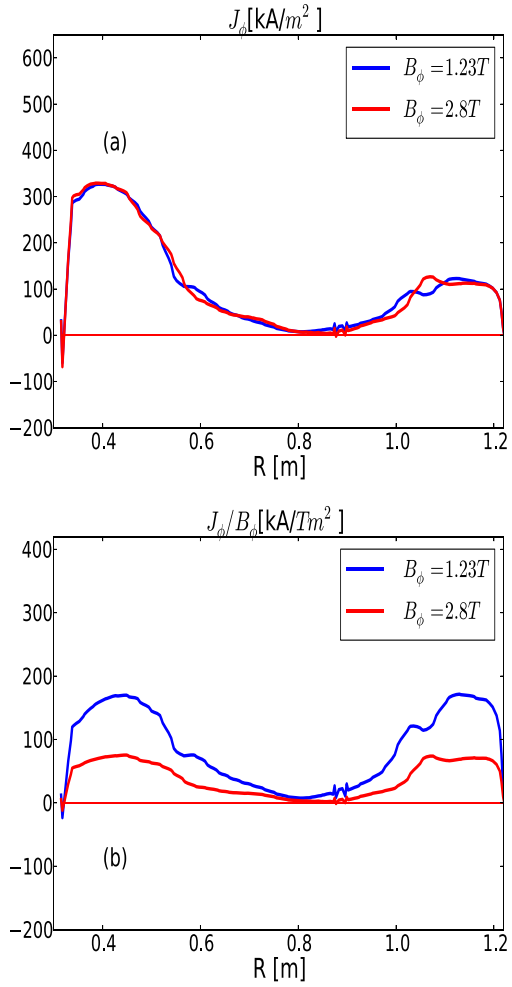

FIG. 9. (a) Current density profiles at t = 8.4 ms (at Z = 0.75 m), for the two cases shown in Fig. 8. (b) and profiles of J_ϕ/B_ϕ, the free energy for current-driven instability.

of 3-D nonaxisymmetric perturbations, these current-carrying axisymmetric (n = 0) smaller-scale plasmoids can first form during a fast reconnection process, while twisted open field lines are being injected and can then merge to form a large current-carrying magnetic bubble for plasma startup in a tokamak. The effect of nonaxisymmetric perturbations, and the onset of nonaxisymmetric current-sheet instabilities ($n \neq 0$ modes) and their effect on flux closure for an effective current startup are also studied as the toroidal guide field was increased. It is found that while axisymmetric 2-D current-carrying plasmoids are formed at an arbitrary toroidal guide field, 3-D nonaxisymmetric current-sheet instabilities (edge filaments) can be triggered, but could be completely stabilized at a higher toroidal guide field.

Results presented here are consistent with transient CHI experiments in NSTX.[16] Camera images in NSTX have shown axisymmetric closed flux formation during transient CHI and have not detected persistent nonaxisymmetric fluctuations or filament formation. This highlights the advantage of transient CHI in large spherical tokamaks. First, the toroidal guide field in spherical tokamaks helps to mitigate or stabilize edge nonaxisymmetric fluctuations. Also, a closed flux plasma current is formed at a higher current multiplication factor (the ratio of the plasma current to the injector current). Second, unlike conventional driven CHI where the injector voltage is applied throughout the discharge, in transient CHI, voltage is turned off after flux expansion in the vessel. This limits the role of edge nonaxisymmetric modes, and as shown in the simulations, 3-D fluctuations can decay. It should be noted that for driven CHI, or at higher edge Lundquist numbers when fluctuations saturate at higher amplitudes, the relaxation of edge current-driven peeling filaments could go through relaxation cycles due to a fluctuation-induced dynamo term.[28] However, in transient CHI, the goal is to achieve ohmically self-heated plasma formation via the generation of large axisymmetric plasma current in the absence of 3-D fluctuations. The 3-D results presented here support this scenario at a high toroidal flux.

As next-step Spherical Tokamak (ST) devices will operate at both higher toroidal flux and injector poloidal flux, three-dimensional MHD simulations are critical and essential for prediction and accessibility to these regimes of maximum start-up current in larger STs, such as ST-FNSF (Fusion Nuclear Science Facility). Our 3-D simulations presented here show the promising results that transient CHI, a leading technique for a noninductive startup current drive in spherical tokamaks, could be scalable to a higher poloidal injector flux, as well as toroidal flux. Previous axisymmetric NIMROD simulations have shown that CHI generated plasma current scales directly with the injector poloidal flux.[20] It is therefore expected that by injecting larger flux, larger plasma current up to 1 MA can be obtained. This has also been shown in the axisymmetric Tokamak Simulation Code (TSC) simulations.[33] However, further 3-D MHD stability analysis and optimization, at both higher poloidal injection flux up to 1 Wb and higher toroidal flux to achieve MA current startup via transient CHI, are needed and will be presented in a future study.

Finally, helicity injection experiments in laboratory fusion configurations, which are primarily intended to generate plasma current as a fusion application, can also provide a very rich platform for studying magnetic reconnection in the absence of pre-existing instabilities (kink or tearing). Understanding the physics of magnetic reconnection during CHI is of great importance for the success of this technique as a noninductive plasma start-up and ultimately for steady-state current drive, a necessity for a viable reactor design. On the other hand, plasmoid-mediated magnetic reconnection during CHI exhibits both fast reconnection and global system-size plasmoid formation. These rich characteristics have placed CHI plasma start-up in tokamaks on the phase diagram for magnetic reconnection in the collisional to weakly collisionless regimes, with the possibility of transitioning from single X-line to multiple X-line.[34]

In summary, important highlights of our 3-D global numerical study presented here are (1) fast reconnecting current-carrying axisymmetric (n = 0) plasmoids are formed even in the presence of 3-D nonaxisymmetric perturbations, and at an arbitrary toroidal guide field, (2) 3-D nonaxisymmetric current-sheet instabilities ($n \neq 0$ edge modes) can be triggered, but can be completely stabilized at a higher toroidal guide field. Our simulations show that 3-D perturbations arising from neighboring outer edge $n \neq 0$ current-sheet instabilities, if present, could contribute to an enhancement of global magnetic reconnection for the formation of current-carrying axisymmetric (n = 0) plasmoids, which ultimately merge to form a large solenoid-free axisymmetric plasma current for startup in a tokamak.

ACKNOWLEDGMENTS

The authors thank R. Raman and S. Kaye for useful discussions. Computations were performed at NERSC and local PPPL cluster. This work was supported by DOE Grant Nos. DE-AC02-09CH11466 and DE-SC0010565.

The digital data for this paper can be found at http://arks.princeton.edu/ark:/88435/dsp011v53k0334.

REFERENCES

[1]M. A. Berger and G. B. Field, J. Fluid Mech. **147**, 133 (1984).
[2]P. M. Bellan, *Magnetic Helicity, Spheromaks, Solar Corona Loops, and Astrophysical Jets* (World Scientific Publishing Co, 2018).
[3]E. G. Blackman, Space Sci. Rev. **188**, 59 (2015).
[4]K. Kusano, T. Maeshiro, T. Yokoyama, and T. Sakurai, Astrophys. J. **577**, 501 (2002).
[5]P. Démoulin and E. Pariat, Adv. Space Res. **43**, 1013 (2009).
[6]F. Ebrahimi and R. Raman, Phys. Rev. Lett. **114**, 205003 (2015).
[7]M. Ono, C. B. Forest, Y. Hwang, R. Armstrong, W. Choe, G. Greene, T. Jones, T. Jarboe, A. Martin, B. Nelson *et al.*, in *Proceedings of the 14th International Conference on Plasma Physics and Controlled Nuclear Fusion Research 1992*, Würzburg (IAEA, 1993), p. 693.
[8]M. Ono, S. M. Kaye, Y.-K. M. Peng, G. Barnes, W. Blanchard, M. D. Carter, J. Chrzanowski, L. Dudek, R. Ewig, D. Gates *et al.*, Nucl. Fusion **40**, 557 (2000).
[9]F. Ebrahimi, S. C. Prager, J. S. Sarff, and J. C. Wright, Phys. Plasmas **10**, 999 (2003).
[10]K. J. McCollam, J. K. Anderson, A. P. Blair, D. Craig, D. J. den Hartog, F. Ebrahimi, R. O'Connell, J. A. Reusch, J. S. Sarff, H. D. Stephens *et al.*, Phys. Plasmas **17**, 082506 (2010).
[11]D. J. Battaglia, M. W. Bongard, R. J. Fonck, and A. J. Redd, Nucl. Fusion **51**, 073029 (2011).
[12]P. K. Browning, A. Stanier, G. Ashworth, K. G. McClements, and V. S. Lukin, Plasma Phys. Controlled Fusion **56**, 064009 (2014).
[13]T. R. Jarboe, I. Henins, A. R. Sherwood, C. W. Barnes, and H. W. Hoida, Phys. Rev. Lett. **51**, 39 (1983).
[14]T. R. Jarboe, Fusion Technol. **15**, 7 (1989).
[15]R. Raman, T. R. Jarboe, B. A. Nelson, V. A. Izzo, R. G. O'Neill, A. J. Redd, and R. J. Smith, Phys. Rev. Lett. **90**, 075005 (2003).
[16]R. Raman, B. A. Nelson, M. G. Bell, T. R. Jarboe, D. Mueller, T. Bigelow, B. Leblanc, R. Maqueda, J. Menard, M. Ono *et al.*, Phys. Rev. Lett. **97**, 175002 (2006).
[17]R. Raman, D. Mueller, B. A. Nelson, T. R. Jarboe, S. Gerhardt, H. W. Kugel, B. Leblanc, R. Maingi, J. Menard, M. Ono *et al.*, Phys. Rev. Lett. **104**, 095003 (2010).
[18]K. Kuroda, R. Raman, K. Hanada, M. Hasegawa, T. Onchi, M. Ono, B. A. Nelson, T. R. Jarboe, M. Nagata, O. Mitarai *et al.*, Plasma Phys. Controlled Fusion **60**, 115001 (2018).
[19]F. Ebrahimi, E. B. Hooper, C. R. Sovinec, and R. Raman, Phys. Plasmas **20**, 090702 (2013).
[20]F. Ebrahimi, R. Raman, E. B. Hooper, C. R. Sovinec, and A. Bhattacharjee, Phys. Plasmas **21**, 056109 (2014).
[21]F. Ebrahimi and R. Raman, Nucl. Fusion **56**, 044002 (2016).
[22]D. Biskamp, Phys. Fluids **29**, 1520 (1986).
[23]*Plasma Astrophysics*, edited by T. Tajima and K. Shibata (Addison-Wesley, 1997).
[24]N. F. Loureiro, A. A. Schekochihin, and S. C. Cowley, Phys. Plasmas **14**, 100703 (2007).
[25]W. Daughton, V. Roytershteyn, B. J. Albright, H. Karimabadi, L. Yin, and K. J. Bowers, Phys. Rev. Lett. **103**, 065004 (2009).
[26]L. Comisso, M. Lingam, Y.-M. Huang, and A. Bhattacharjee, Phys. Plasmas **23**, 100702 (2016).
[27]F. Ebrahimi, Phys. Plasmas **23**, 120705 (2016).
[28]F. Ebrahimi, Phys. Plasmas **24**, 056119 (2017).
[29]E. Hooper and C. Sovinec, Phys. Plasmas **23**, 102502 (2016).
[30]B. I. Cohen, C. A. Romero-Talamás, D. D. Ryutov, E. B. Hooper, L. L. LoDestro, H. S. McLean, T. L. Stewart, and R. D. Wood, Phys. Plasmas **16**, 042501 (2009).
[31]C. R. Sovinec, A. H. Glasser, T. A. Gianakon, D. C. Barnes, R. A. Nebel, S. E. Kruger, D. D. Schnack, S. J. Plimpton, A. Tarditi, M. Chu *et al.*, J. Comput. Phys. **195**, 355 (2004).
[32]E. B. Hooper, C. R. Sovinec, R. Raman, F. Ebrahimi, and J. E. Menard, Phys. Plasmas **20**, 092510 (2013).
[33]K. C. Hammond, R. Raman, and S. C. Jardin, Phys. Plasmas **26**, 032501 (2019).
[34]H. Ji and W. Daughton, Phys. Plasmas **18**, 111207 (2011).